Research Paper

Application of a UHPLC-MS/MS method to investigate the metabolic pathways of Alzheimer's disease and dementia with Lewy bodies using postmortem cerebrospinal fluid and serum samples

Yoshio Muguruma[1], Haruhito Tsutsui[1,2], Yoshio Hashizume[3], Hiroyasu Akatsu[3,4], Koichi Inoue[1]*

[1]Graduate School of Pharmaceutical Sciences, Ritsumeikan University, 1−1−1 Nojihigashi, Kusatsu, Shiga 525−8577, Japan
[2]ONO Pharmaceutical Co., Ltd, 3−1−1 Sakurai, Shimamoto-cho, Mishima-gun, Osaka 618−8585, Japan
[3]Department of Neuropathology, Choju Medical Institute, Fukushimura Hospital, Toyohashi, Aichi 441−8124, Japan
[4]Department of Medicine for Community-Based Medical Education, Nagoya City University Graduate School of Medical Sciences, Nagoya, Aichi 467−0001, Japan

Abstract Metabolic pathways are potential diagnostic markers for the early diagnosis of age-related cognitive decline due to Alzheimer's disease (AD) and dementia with Lewy bodies (DLB). Investigating the minute fluctuations of metabolite concentration or the ratios in cerebrospinal fluid (CSF) and serum that are reflected in brain disorders could lead to identify a useful biomarker candidate for the differential diagnosis between AD and DLB. Most metabolites are hydrophilic, so they were measured as 9-fluorenylmethyl chloroformate (FMOC) derivatives simultaneously using a liquid chromatography based on C18 column. The aim of this study was to validate and apply a simple and effective ultra-high performance liquid chromatography-tandem mass spectrometry (UHPLC-MS/MS) method for the simultaneous determination of metabolites in CSF and serum samples from AD and DLB patients with confirmed diagnoses based on brain pathology. To evaluate the diversity of ninety-nine amine-mediated metabolic patterns and pathways, we identified possible metabolites that contributed to and mutually influenced principal component analysis with integrated analytes. The concentrations of several analytes differed significantly between the AD and DLB groups. The trends in the concentrations of intermediates in the amine metabolic pathway indicated an increase or decrease in β-alanine metabolism. The common metabolic patterns in the CSF and serum of AD and DLB patients included elevated levels of cystathionine, 3-hydroxykynurenine, 3-methoxytyramine, N^G,N^G-dimethyl-L-arginine, glutamate, uracil, and polyamines. The concentrations of cadaverine, arginine, and acetyllysine were lower. The results of our metabolic pathway analysis indicated that neurodegeneration would be involved peripheral β-alanine metabolites. Assessing comprehensively several metabolites identified using widely targeted metabolomics as multi-biomarker candidates would be effective technique to provide novel insights on neuroscience research.

Key words: widely targeted metabolomics, Alzheimer's disease, dementia with Lewy bodies, 9-fluorenylmethyl chloroformate, UHPLC-MS/MS

* **Corresponding author**
Koichi Inoue
Laboratory of Clinical & Analytical Chemistry, Graduate School of Pharmaceutical Sciences, Ritsumeikan University, 1−1−1 Nojihigashi, Kusatsu, Shiga 525−8577, Japan
Tel: +81−77−561−5838, Fax: +81−77−561−2564
E-mail: kinoue@fc.ritsumei.ac.jp
Received: October 7, 2020. Accepted: January 2, 2021.
Epub March 3, 2021.
DOI: 10.24508/mms.2021.06.002

1. Introduction

Diseases that cause dementia are roughly divided into four categories: Alzheimer's disease (AD), dementia with Lewy bodies (DLB), cerebrovascular dementia, and frontotemporal dementia. AD and DLB are the most common neurodegenerative diseases. The consensus guidelines developed by the National Institute on Aging Alzheimer's Association (NIA-AA) are currently the most widely used clinical criteria for AD assessment[1,2]. A high-probability

AD diagnosis is enabled by a combination of clinical characteristics and the verified presence of indicative biomarkers. These include β-amyloid 1−42 ($A\beta_{1-42}$) and/or phosphorylated tau (p-tau) in the brain, which are detected via amyloid positron emission tomography (PET) and magnetic resonance imaging (MRI)[3−5]. Moreover, in the CSF, These protein markers are quantitatively analyzed with a high-sensitivity Enzyme-Linked Immunosorbent Assay or Immunoprecipitation-mass spectrometry[6,7]. The diagnostic criteria for DLB defined by McKeith and the DLB consortium include decreased uptake by dopamine transporters in the basal ganglia, which is confirmed via PET or single photon emission computed tomography, and reduced [^{123}I]-metaiodobenzylguanidine (MIBG) uptake during myocardial scintigraphy imaging[8−10]. However, these clinical tests are not practical in the early stages of dementia, because they are expensive, invasive, time-consuming, and lack the necessary sensitivity. It is thus important to develop bioanalytical techniques for the objective assessment of dementia type.

AD and DLB have heterogeneous clinical and pathologic phenotypes that often overlap, so serious misdiagnosis occasionally occurs. It is particularly difficult to identify patients who are confused because DLB-related pathology has been overlooked[11−13]. Although these neurodegenerative diseases have similarities, the proteinopathies caused by AD and DLB differ. The etiology of AD is associated with pathologic $A\beta$ and tau protein aggregation, while DLB is α-synuclein protein aggregation. The metabolic changes in biological samples will be undoubtedly reflected in the difference of these protein aggregates that cause AD or DLB. Identifying altered metabolism in the central nervous system (CNS), including the brain and CSF, would facilitate the direct association of observed premortem brain pathology with related neurological AD and DLB disorders. On the other hand, the practical candidate markers in blood samples for simple clinical diagnosis is also required.

The metabolite concentrations in biological fluids fluctuate significantly as neurodegenerative disease progresses, which is due to changes in the activities and concentrations of metabolic enzymes. It has been reported that the brain tissues of DLB patients contain lower levels of the noradrenaline (NA) metabolite 3-methoxy-4-hydroxyphenylglycol (MHPG) than the brain tissues of AD patients[14,15]. Measuring the amounts of MHPG and/or NA in the CSF and serum of AD and DLB patients can significantly improve the accuracy of differential diagnosis. To the best of our knowledge, no other metabolites in human biological fluids that would facilitate the differential diagnosis of AD and DLB have been identified. Metabolomics technology can thus be a powerful tool to detect altered low-molecular-weight metabolites that are closely associated with AD and DLB pathogenesis.

Metabolomics methods that employ ultra-high performance liquid chromatography and tandem mass spectrometry (UHPLC-MS/MS) in selected reaction monitoring (SRM) mode are used widely to rapidly and effectively separate a wide range of neurochemicals. However, reversed-phase LC columns retain highly polar metabolites poorly, and the sensitivity of MS detection is low. To overcome these limitations, chemical reagents have recently been developed to derivatize $-NH_2$, −COOH, and −SH functional groups for the simultaneous quantitative analysis of biological samples[16−19]. 9-Fluorenylmethyl chloroformate (FMOC) is a well-known labeling reagent that reacts immediately with primary and secondary amines under alkaline conditions to form stable complexes. Sánchez-López et al. developed an LC-MS method that included FMOC derivatization to detect 35 polar amino acids and amines in plasma samples[20]. We previously reported on FMOC derivatization as an effective strategy for the detection of a wide range of amine metabolites. FMOC derivatization increased the sensitivity of MS detection in positive electrospray ionization (ESI) mode and improved chromatographic features, including peak shape and retention time on reversed-phase UHPLC columns[21]. Our multi-analyte method provided a broad view of the metabolic pathways involving amines in CSF and serum. Determining the comprehensive metabolomic signatures of endogenous metabolites enabled us to better understand the pathological status and neurodegenerative mechanisms caused by metabolic disorders. High-throughput UHPLC-MS/MS assays and derivatization are thus essential for the simultaneous quantitative analysis of target metabolites to differentiate between AD and DLB.

Profiling metabolic pathways for the differential diagnosis of dementia must consider multiple combinations that reflect the direct and indirect effects of the CNS on brain tissue. However, it is not possible to use biopsied brain tissue for clinical diagnosis in the early stages of dementia. A combination of strategies, including neuropsychological testing, imaging, and omics analysis, is recommended for

the identification of suitable and distinctive CNS metabolites to diagnose dementia[22,23]. The metabolomic analysis of CSF and/or serum can provide insight into neurodegenerative processes and facilitate the identification of potential biomarkers to differentiate between AD and DLB. In this study, we conducted the metabolomic analysis with a focus on endogenous aminergic metabolites using validated a UHPLC-MS/MS method with FMOC derivatization. The method was applied to investigate amine-mediated metabolic patterns in CSF and serum samples from patients with confirmed AD- and DLB-related pathologies. We also performed bivariate and multivariate analysis to identify potential AD and DLB markers for differential diagnosis.

2. Materials and Methods

2.1. Chemicals and reagents

Ninety-nine target metabolites and thirty-three internal standards (ISs) were used for our comprehensive metabolic analysis (Fig. 1). Detail analytical standards and abbreviations were shown in Supplementary data. 9-Fluorenylmethyl chloroformate (FMOC), sodium hydrogen carbonate ($NaHCO_3$), distilled water, and HPLC grade ethanol, acetonitrile, and formic acid (FA) were obtained from Fujifilm Wako Pure Chemical Co. (Osaka, Japan) and used to derivatize the target amines. Purified water used throughout the study was obtained from a PURELAB Flex 5 system (ELGA, London, UK).

2.2. FMOC derivatized UHPLC-MS/MS analysis

The instrumental methodology was previously reported for the metabolic analysis of CSF samples[21]. The detailed LC-MS methodology including the column, the mobile phase, the gradient condition, the derivatization process, and the SRM transitions of the 99 analytes and 33 ISs are summarized in Supplementary information and Table S1.

2.3. Biological information

The bioanalysis included fifteen individuals who underwent accurate, reliable, and detailed pathological evaluations. Five of the subjects were diagnosed with AD, and five were diagnosed with DLB. The study was confined to patients who had been diagnosed with gradual premortem memory loss, and plaques, tangles, and/or Lewy bodies were observed in the brain. Characteristic senile plaques (SPs) and neurofibrillary tangles (NFTs) were evaluated based on their three-stage (*A*, *B*, *C*) and six-stage (*I–VI*) Braak scores, respectively. Lewy body was classified as either limbic type or neocortical type based on their distributions. All human CSF and serum samples from AD patients 76 to 92 years of age and DLB patients 81 to 94 years of age were provided by the Fukushimura Brain Bank at Fukushimura Hospital. We obtained informed consent in writing from the patients' guardians to have autopsies per-

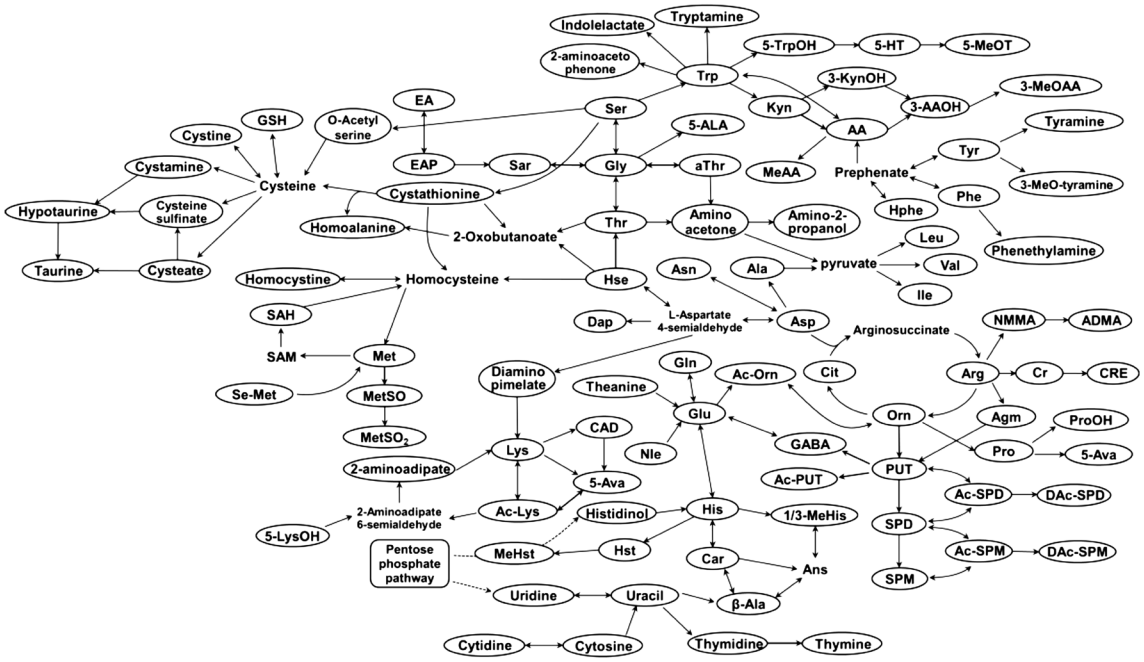

Fig. 1. Metabolic pathways for amine and amino acid metabolites based on the KEGG PATHWAY database.

Table 1. Biological information

Groups	No.	Age	Sex	SP Braak stage	NFT Braak stage	Brain fix (h)	Pathological diagnosis
DLB	1	94	Female	C	III	3	Limbic type
	2	82	Male	B	II	3	Limbic type, CAA (medium)
	3	85	Female	C	III	2	Neocortical type
	4	81	Male	B	II	2	Neocortical type
	5	86	Female	B	IV	2	Neocortical type, CAA (medium)
AD	1	88	Male	C	IV	No data	CAA (light), *α*-synuclein (+)
	2	92	Female	C	VI	12.5	CAA (light), *α*-synuclein (−)
	3	80	Male	C	VI	10	CAA (medium), *α*-synuclein (−)
	4	87	Female	C	V	18	No data
	5	76	Male	C	VI	2	CAA (medium), *α*-synuclein (−)
Control	—	85	Male	A	I	2.5	CAA (heavy), Multiple infarction,
	—	96	Female	(−)	II−III	3	Lewy body(−), Multiple infarction, Arteriosclerosis
	—	86	Male	A	I	3	Lewy body(−), CAA(−),
	—	76	Male	(−)	I	3.5	*α*-synuclein (−), Multiple cerebral infarction
	—	85	Female	(−)	(−)	4	Cervical spondylotic myelopathy, Tau deposition

Bottom note: CAA: cerebral amyloid angiopathy, SP: senile plague, NFT: neurofibrillary tangle.

formed and permission to publish the diagnostic and research results. Detailed information about the participants, including age, gender, and the severity of SP and NFT progression is summarized in Table 1.

2.4. Pretreatment of CSF and serum samples

Samples containing 2 mL each were obtained from the AD and DLB subjects. Following the ethical approval by the Ritsumeikan University ethics panel (No. BKC-IRB-2015-012), the samples were gently divided into −1.0 mL aliquots in collection tubes and stored in a −80°C freezer until analyzed. Aliquots of CSF and serum (200 μL) from the AD and DLB patients were transferred into 2.0 mL microcentrifuge tubes and spiked with 20 μL of the mixed IS solution and 180 μL of acetonitrile. The mixtures were vigorously vortexed for 30 s and centrifuged in a CF15RN centrifuge (Hitachi, Tokyo, Japan) at 15,000 rpm (21,200 × *g*) for 5 min at 4°C to remove proteins. After centrifugation, 300 μL of each supernatant was subjected to FMOC derivatization as described in Section 2.3. The solvent was then removed from the reaction mixtures again using a centrifugal evaporator. The residues were dissolved in acetonitrile (75 μL) and centrifuged at 15,000 rpm for 5 min to remove salts, and 50 μL aliquots of the supernatants were mixed with 50 μL aliquots of 0.2% FA in water. The solutions were vortexed, and 5 μL of each sample was used for UHPLC-MS/MS analysis.

2.5. Validation

To validate the UHPLC-MS/MS method with FMOC derivatization, we evaluated specificity, selectivity, limits of detection (LODs), limits of quantitation (LOQs), linearity, and recovery. The use of 33 isotopically labeled ISs minimized error due to analyte loss and the variability of MS detection, which improved analytical performance. Specificity and selectivity were evaluated using the retention time and MS profiles of pure standards. The LODs and LOQs for the amine metabolites were based on the signal-to-noise (*S*/*N*) ratios obtained at the lowest detected concentrations. Calibration curves were constructed by sequentially diluting the stock solutions to concentrations in a fixed range of 1 nM to 100 μM and plotting the ratios of the standard and IS peak areas (y) against the concentrations of the adjusted standard solutions (x, nM). The linear ranges included a minimum of six concentrations. High and low recoveries (%) were calculated according to $F/(F_0+A) \times 100$. F and F_0 are the analyte concentrations in the spiked and unspiked samples, respectively, and A is the spike concentration. The same researcher analyzed the CSF and serum samples over a short period of time at room temperature to determine repeatability.

2.6. Data analysis

Data acquisition and analysis were performed using MassLynx 4.1 (Waters Co., Milford, MA, USA), and Tar-

getLynx software was used for data processing to construct the calibration curves and calculate sample concentrations. The quantitative data are reported as the mean±standard deviation (SD) obtained from two biological samples. The means and SDs were determined using Microsoft Excel software (version 1908, Microsoft) and compared by performing Student's *t*-tests or Welch's *t*-tests. A calculated *p*-value (<0.05) was selected to indicate statistical significance in every comparison. The measured β-Ala peripheral metabolite concentrations in DLB and AD samples were normalized, exported, and compared by bivariate and multivariate statistical analysis using MATLAB R2019b (MathWorks, Inc, Natick, MA). A two-dimensional clustering heatmap was constructed to compare correlations in the complex metabolic patterns of CSF and serum from DLB or AD patients. The functional codes (*pdist*, *linkage*, *cophenet*, *dendrogram*, *heatmap*) were used to return and visualize a matrix that encodes a tree that contains a hierarchical cluster of rows of input data matrices. Regression analysis of the receiver operating characteristic (ROC) curves was also performed for binary classification based on metabolic changes in the CSF and serum. The functional codes (*fitglm*, *perfcurve*) were used to return a generalized linear model fit to variables in the table or dataset array. We used the areas under the ROC curves (AUCs) to evaluate the diagnostic accuracy of the metabolic profiles. Principal component analysis (PCA) of the target metabolite data was conducted to obtain multivariate statistical models to classify AD and DLB pathology statistically. The functional codes (*pca*) was used to find the principal components for the ingredients data. The mean value was substituted for missing values.

3. Results and Discussion

3.1. Optimization of the highly sensitive and selective targeted metabolomics method with FMOC derivatization

The simultaneous analysis of endogenous metabolites in a single run remains a major challenge in the field of targeted metabolomics, particularly for metabolites present in low abundance or across a wide range of concentrations. To analyze the profiles of amine metabolites in human biological samples, we searched the Human Metabolome Database (HMDB)[24] and pathway databases, including the Kyoto Encyclopedia of Genes and Genomes (KEGG)[25], to select our target compounds (Fig. 1). We then optimized the method for a wide range of target metabolites. We aimed to expand on our previous work and develop a reliable and rapid analytical method to quantify the vast number of amine metabolites in biological samples using UHPLC-MS/MS. To simultaneously quantify endogenous metabolites with different chemical properties, we employed amine-selective FMOC derivatization and optimized the reaction conditions, reaction time, and temperature to obtain high yields[21]. Optimal FMOC derivatization was achieved with a reaction time of 10 min at room temperature. For sensitive and selective detection of the target metabolites, we investigated their MS fragmentation patterns and determined the precursor and product transitions by varying the cone voltage or collision energy. Most of analytes were detected as mono-protonated derivatives ($[M+H]^+$). A product ion derived from the FMOC reagent moiety (*m*/*z* 179) was selectivity generated during collision-induced dissociation in the tandem MS. We thus selected this SRM transition to analyze most of the metabolites in positive ESI mode. Specific product ions of Tau and cysteate were observed at *m*/*z* 124 and *m*/*z* 112, respectively, in negative ESI mode. The ESI-MS/MS conditions tested for the FMOC amine derivatives are listed in Table S1. After identifying the optimal FMOC derivatization and MS conditions, we were able to analyze 99 target metabolites in 10 minutes. Quantifying a wide range of target metabolites enabled us to assess variations in the amine metabolic pathways in various human body fluids.

3.2. Method validation using CSF and serum samples: LOQs, LODs, linearity, and recovery

The quantification assay was validated for the analysis of biologically active metabolites in human CSF and serum in terms of the LODs, LOQs, linearity, and recovery. The LOQs and LODs of the metabolites were in the nM range. The estimated LOQs (*S*/*N*=10) ranged from 1 to 1,000 nM, and the LODs (*S*/*N*=3) ranged from 0.1 to 500 nM. These results indicated that the assay was sensitive to detect trace levels of the metabolites in CSF and serum. Calibration curves were prepared by plotting concentration (nM) on the *x*-axis and the derivative/IS peak area ratio on the *y*-axis. The linearity of the standard calibration curves in the quantification range from 1 nM to 100 μM was investigated by constructing calibration curves that included at least six different concentrations. The linear ranges for most of the ana-

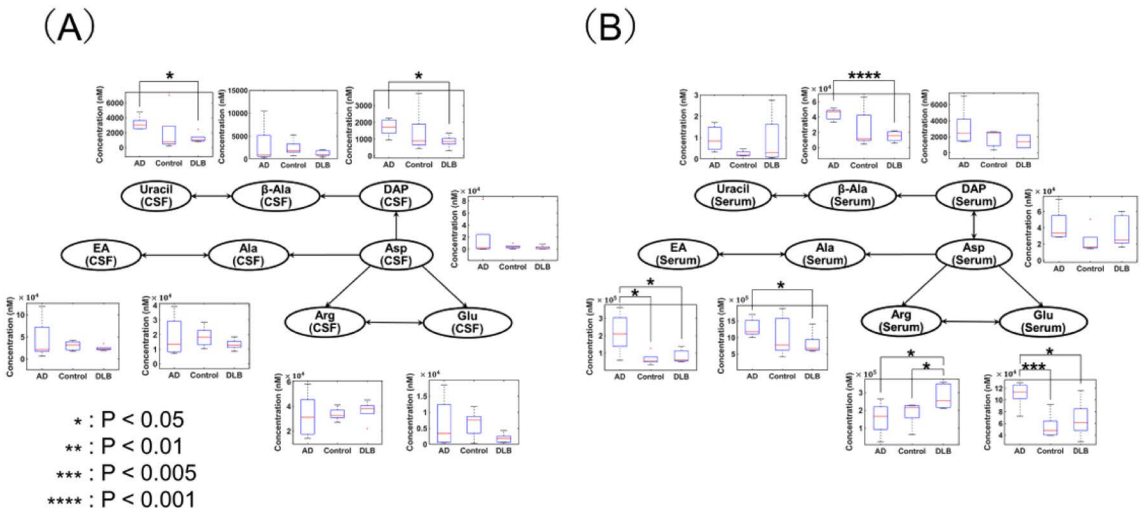

Fig. 2. Detailed metabolic variations in *β*-alanine metabolism observed in (A) CSF and (B) serum collected from AD and DLB patients.

$^{*}P<0.05$, $^{**}P<0.01$, $^{***}P<0.005$, $^{****}P<0.001$. The color gradients indicate higher (red) or lower (blue) concentrations calculated by diving the median (AD/DLB).

lytes were spanned more than two orders of magnitude, and all of the standard curves had high correlation coefficients in the range of 0.990 to 1.000 when $1/x$ was used as a weighting factor. 33 out of 99 analytes were measured after diluting the CSF and serum samples ten-fold. However, the concentrations of Gln in CSF and Ala, ProOH, Asn, Glu, Ac-Orn, uridine, Lys, and cystathionine in serum were exceeded the upper limit of the calibration range. Analyte recovery and reproducibility were evaluated by spiking the standard solution in 180 μL of pooled CSF and serum (n=6). The validation results of human CSF samples were reported previously[21]. Good recoveries from serum after 10-fold dilution were obtained for 57 of the 99 compounds (Supporting Information, Table S3). Recoveries from CSF (10−10,000 nM) and serum (1,000−10,000 nM) ranged from 44.9 to 121.3% and from 67.7 to 117.8%, respectively. The precision of the recovery is reported as the coefficient of variation, CV (%). Precision was within 11.5% at each concentration. We prepared 33 isotopically labeled ISs for the study, although this was an insufficient number for a robust analysis. Therefore, we are currently investigating additional ISs. The detailed method validation data are shown in Table S2 and Table S3.

3.3. Widely targeted metabolomic analysis of CSF and serum from DLB and AD patients

Based on differences between the pathological characteristics of DLB and AD, metabolic variations could be expected in biological samples to discriminate between the two types of dementia. Widely targeted metabolomics assay revealed how metabolites in the DLB and AD groups were affected by the respective pathologic phenotypes, which could be useful for the differential diagnosis of DLB and AD. The method was used to analyze 15 CSF and serum samples from patients with AD (n=5), DLB (n=5) and Control (n=5). Typical standard and CSF UHPLC-ESI-MS/MS chromatograms are shown in our previous report [21]. Chromatograms of all the target analytes in serum analyzed in this study are presented in Fig. S1. We quantified more than 70 of the 99 biologically active metabolites in both CSF and serum samples collected from AD and DLB patients (Table S4). Metabolic pathway analysis made it possible to visualize the biochemical relationships between amine metabolism in the CSF and serum samples (Fig. S2, Fig. S3). Statistically significant differences between the concentrations of seven peripheral *β*-Ala metabolites were indicated by p-values below 0.05 in Student's t-tests or Welch's t-tests. (Fig. 2). Similar metabolic patterns observed in the CSF and serum of AD and DLB patients included increased concentrations of cystathionine, 3-KynOH, 3-MeO-tyramine, ADMA, Glu, uracil, and polyamines. The concentrations of CAD, Arg, and Ac-Lys were reduced. The median ratios and p-values of the metabolites in the CSF and serum samples that reflected similar metabolic patterns are listed in order in Table 2. The significance of differences between the seven compounds was evaluated in subsequent statistical analyses.

To assess the seven metabolites as CSF and serum possi-

Table 2. List of significant changes in metabolites in CSF or serum from AD vs DLB

Analytes	CSF			Serum		
	Ratio	*p*-value		Ratio	*p*-value	
EA	0.97	0.37	—	3.54	0.04	*
β-Ala	0.88	0.37	—	2.97	0.0002	****
Ala	1.05	0.42	—	1.76	0.04	*
Uracil	2.86	0.01	*	2.81	0.90	—
Glu	1.82	0.36	—	1.84	0.04	*
3-MeO-tyramine	2.17	0.06	—	3.56	0.30	—
Arg	0.82	0.69	—	0.66	0.05	*
Ac-Lys	0.66	0.53	—	0.51	0.27	—
ADMA	1.67	0.68	—	2.09	0.49	—
DAP	1.96	0.03	*	1.72	0.38	—
CAD	0.32	0.62	—	0.56	0.65	—
Cystathionine	1.88	0.38	—	2.19	0.32	—
3-KynOH	2.31	0.57	—	9.12	0.10	—
SPD	1.60	0.41	—	1.30	0.58	—
Ac-SPM	2.88	0.36	—	1.70	0.90	—
SPM	1.72	0.38	—	4.08	0.15	—

"Ratio" is the comparative value of the median (AD/DLB). The *p*-value was calculated using Student *t*-test or Welch's *t* test (*$p<0.05$, **$p<0.01$, ***$p<0.005$, ****$p<0.001$).

ble biomarker candidates, we performed bivariate and multivariate statistical analysis and built models to differentiate between the AD and DLB groups. The concentration of each compound in CSF and serum was normalized by subtracting the mean concentration from the absolute concentration and dividing the resulting value by the SD. The heatmaps of the DLB and AD groups based on the normalized metabolite concentrations in CSF (Fig. 3A) and serum (Fig. 3B) were created. The estimated amounts of peripheral β-Ala metabolites in the CSF and serum of AD patients were higher than those estimated for DLB patients. The concentrations of uracil and DAP in CSF were 2.9 and 2.0 times higher, respectively, and the differences were statistically significant. The β-Ala concentration in serum was three times higher. Hierarchical clustering analyses was performed to obtain respective profiles between the samples and between the seven analytes. With the exception of AD sample No. 2 (CSF), the samples were divided between an AD cluster and a DLB cluster. Although we suspected that the EA, Ala, and β-Ala concentrations were slightly correlated, there was no obvious relationship between the seven analytes based on the metabolic pathway (Fig. 3A, 3B). We chose to perform PCA analysis, because it reduced the dimensionality of the data. This allowed us to discriminate between the variances of the samples and identify cluster outliers. The PCA results for the seven metabolites are shown in Fig. 3C and 3D. In the first principal component plot, the horizontal (*x*) axis effectively and distinctly separated the two groups according to the identified metabolites. This result was significant, because it indicated that the metabolic profiles of biofluids from AD and DLB patients differed. The seven metabolites could thus serve as possible biomarker candidates for differential diagnosis. ROC curves and AUC values are widely used to evaluate the performance of diagnostic and prognostic assays. We thus performed ROC analysis for binary classification using the significant biomarker candidates to discriminate between DLB and AD (Fig. 4A and 4B). Uracil in CSF and β-Ala in serum had the best AUC values, which reached 1.00. The AUC values of the others were also above 0.84. The results of bivariate and multivariate statistical analysis, including the heat maps, hierarchical clustering, ROC curves, and PCA collectively indicated that β-Ala metabolites in CSF and serum could be used as possible biomarker candidates for the differential diagnosis of DLB and AD.

3.4. β-alanine metabolism

β-Ala is largely present in the brain and muscles. It is an endogenous β-amino acid and a core metabolic precursor for various metabolic pathways such as pyrimidine, β-Ala,

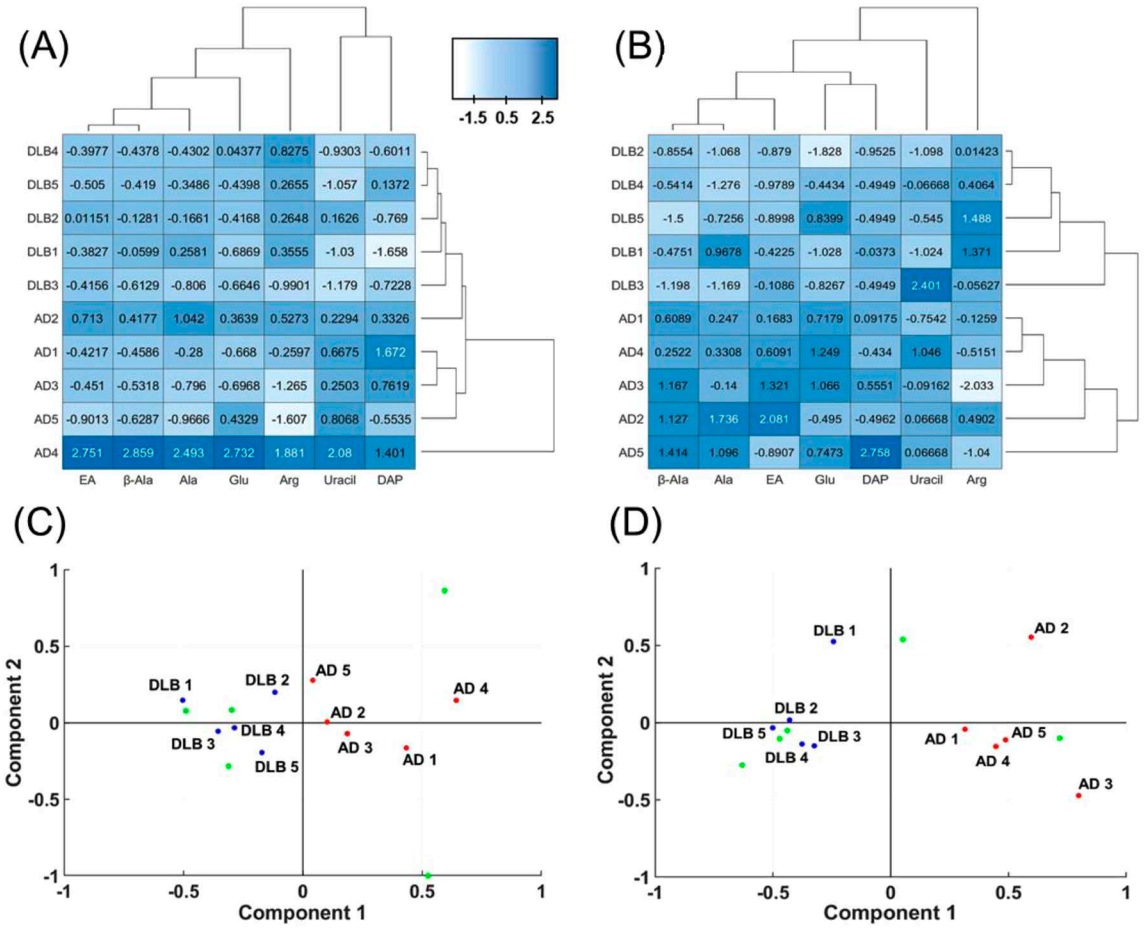

Fig. 3. Multivariate statistical analysis to discriminate between dementia types.
Heatmap and hierarchical clustering analyses to compare peripheral β-Ala metabolic differences between (A) CSF and (B) serum from AD and DLB patients. Values in the heatmap were calculated by subtracting the mean concentration from the absolute concentration and dividing the resulting value by the SD. Samples listed on the vertical axis correspond to the samples in Table 1 (DLB No. 1 to DLB No. 5; blue, AD No. 1 to No. 5; red and controls; green). PCA score plots based on peripheral β-Ala metabolites in (C) CSF (2 kinds) and (D) serum (5 kinds) obtained using MATLAB R2019b software. The DLB samples, AD samples were clearly distinguished by the first principal component (*x*-axis). The contribution ratios of principal component 1 (PC1) and principal component 2 (PC2) on the score plot of CSF were 51.57% and 48.43% respectively. The contribution ratios of PC1, PC2 and PC3 on the score plot of serum were 54.38%, 19.25% and 14.85% respectively.

propanoate, and pantothenate metabolism according to the KEGG database. β-Ala is assumed to be present in biofluids, because it has a low molecular weight and can pass through the blood-brain barrier. As expected, β-Ala and the metabolites in the CSF and serum samples were detected and quantified accurately. Tsuruoka et al. showed that the concentration of β-Ala was 2.0-fold higher in the serum of dementia patients[26]. On the other hand, high serum β-Ala levels were significantly associated with a lower risk of AD[27]. The uracil and DAP concentrations in the CSF of AD patients and the β-Ala concentration in the serum of these patients were 2.9-fold, 2.0-fold, and 3.0-fold higher, respectively, than DLB patients. An elevated β-Ala concentration was consistent with the results of another study. β-Ala is important for primary inhibitory neurotransmitters, including GABA and Gly. Neural cell damages in adult mice, including hypoxia, hypoglycemia, ischemia, oxidative stress, and the presence of free radicals, promoted the release of β-Ala[28]. We thus conclude that elevated β-Ala concentrations in CSF and serum might indicate neural cell damage that occurs more frequently in AD patients than DLB patients.

Imidazole dipeptide, a carnosine generated from β-Ala by carnosine synthase, has important roles as an antioxidant and free radical scavenger. It also has an anti-aging effect in human fibroblasts. In the anti-aging mechanism suggested by Hipkiss et al., carnosine binds to a protein that causes aging *in vivo* and reduces the activity of the protein[29].

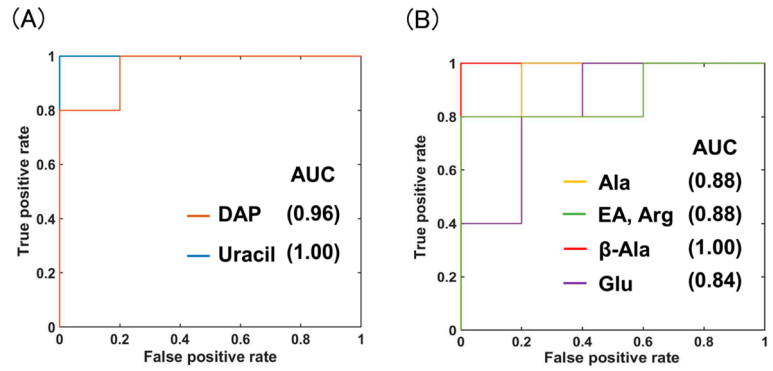

Fig. 4. Differential diagnostic performance based on the ROC curves of significantly different *β*-Ala metabolites.
(A) The CSF markers DAP (AUC=0.96) and uracil (AUC=1.00). (B) The serum markers Ala (AUC=0.88), EA (AUC=0.88), Arg (AUC=0.88), *β*-Ala (AUC=1.00), and Glu (AUC=0.84).

Although they found no significant difference between the carnosine concentrations in the CSF and serum of AD and DLB patients, interestingly, the levels of *β*-Ala and carnosine in CSF and serum samples from DLB patients were lower than they were in samples from AD patients. *β*-Ala and carnosine are also thought to have roles in neuromuscular protection based on changes in calcium sensitivity, which is involved in exercise duration, capacity, and performance[30]. Saunders et al. reported that *β*-Ala supplementation had a significantly positive effect on exercise, and a meta-analysis indicated that the effect was due to an increase in the carnosine concentration in muscle[31]. In short, DLB pathology may cause peripheral neuropathy, which is the one of Parkinsonism that is characterized by bradykinesia, tremor, and muscular rigidity because *β*-Ala and carnosine concentrations decrease. It is necessary for the detection of carnosine in serum to improve LC-MS sensitivity in a future investigation. Accurate quantification using essential or native IS and a large-scale survey of human biofluids from patients with different types of dementia is also needed.

Intriguingly, it has been reported that *β*-Ala-substituted peptides inhibit disease-linked protein aggregation by acting as *β*-sheet breaker, which can reduce the aggregation of *α*-synuclein and other polypeptides associated with diseases due to misfolding. The trimeric *β*-Ala-substituted peptide *β*-Ala-Gln-Lys has also been reported to inhibit A β_{1-40} aggregation[32]. Therefore, bioanalysis to evaluate the association between *β*-Ala-substituted peptides and abnormal brain proteins that cause dementia and identify enzyme deficiencies responsible for metabolic disorders using our widely targeted metabolomics are interesting goals for future work. Also, further metabolomic research of the peripheral *β*-Ala metabolites would lead to identify novel multi-biomarker candidates for differential diagnosis between dementia types.

4. Conclusions

In this study, we developed a sensitive and rapid UHPLC-MS/MS assay to quantify 99 amine metabolites in CSF and serum samples from AD and DLB patients with confirmed diagnoses based on brain pathology. Derivatization with FMOC enabled us to simultaneously separate the metabolites in 10 min and evaluate diverse amine-mediated metabolic patterns and pathways. This method will be useful for identifying neurometabolites that are mirrored in circulating blood and peripheral biomarker candidates that may provide insight into the metabolic behavior of the CNS. This study showed that *β*-Ala metabolism was associated with dementia based on the results of a UHPLC-MS/MS assay. The concentrations of uracil and DAP in the CSF of AD patients and the *β*-Ala concentration in their serum were 2.9 times, 2.0 times, and 3.0 times higher, respectively, than they were in samples from DLB patients. These differences were statistically significant, and they indicated that certain metabolic patterns were affected by pathologies specific to AD and DLB. The data obtained in this study may be highly informative for both widely targeted metabolomics assays and interpreting metabolomic patterns in human samples. In the future, we hope to overcome the limitation of sample size and the challenges using blood samples to differentiate between AD and DLB. We plan to integrate the identification of metabolic patterns using our widely targeted metabolomics method with conventional statistical analyses and artificial intelligence-based technologies.

Acknowledgments

This study was supported by the grants from the Japanese Brain Bank Network for Neuroscience Research, the Ministry of Education, Culture, Sports, Science, and Technology of Japan and JSPS KAKENHI Grant Numbers JP 20J22464. We would like to thank Norihiro Ogawa, Takeshi Kanesaka and Chie Taniguchi for their technical assistance in the clinical and pathological study, and all patients and their guardians for donating the patient organs.

Conflict of Interest

The authors report no conflict of interest.

References

1) McKhann GM, Knopman DS, Chertkow H, Hyman BT, Jack Jr CR, et al: The diagnosis of dementia due to Alzheimer's disease: Recommendations from the National Institute on Aging-Alzheimer's Association workgroups on diagnostic guidelines for Alzheimer's disease. *Alzheimers Dement* 7: 263−269, 2011.
2) Bharadwaj R, Cimino PJ, Flanagan ME, Latimer CS, Gonzalez-Cuyar LF, et al: Application of the condensed protocol for the NIA-AA guidelines for the neuropathological assessment of Alzheimer's disease in an academic clinical practice. *Histopathology* 72: 443−440, 2018.
3) Jennifer LW: Alzheimer's disease neuroimaging. *Curr Opin Neurol* 31: 396−404, 2018.
4) LisaAnn T, Maureen N, Michael DD: Technical Considerations in Brain Amyloid PET Imaging with 18F-Florbetapir. *J Nucl Med Technol* 43: 175−184, 2015.
5) Lisa M, Aneela R, Ivan D, Xian W, Olivia S, et al: Increased Alzheimer's risk during the menopause transition: A 3-year longitudinal brain imaging study. *PLoS One* 13: e0207885, 2018.
6) Sylvain L, Julien D, Xavier A, Cecilia M, Daniel A, et al: Cerebrospinal fluid A beta 1−40 peptides increase in Alzheimer's disease and are highly correlated with phospho-tau in control individuals. *Alzheimers Res Ther* 12: 123, 2020.
7) Erik P, Ann WB, Henrik Z, Kaj B: Determination of beta-amyloid peptide signatures in cerebrospinal fluid using immunoprecipitation-mass spectrometry. *J Proteome Res* 5: 1010−1016, 2006.
8) McKeith IG, Dickson DW, Lowe J, Emre M, O'Brien JT, et al: Diagnosis and management of dementia with Lewy bodies: Third report of the DLB Consortium. *Neurology* 65: 1863−1872, 2005.
9) McKeith IG, Boeve BF, Dickson DW, Halliday G, Taylor JP, et al: Diagnosis and management of dementia with Lewy bodies: Fourth consensus report of the DLB Consortium. *Neurology* 89: 88−100, 2017.
10) McCleery J, Morgan S, Bradley KM, Noel-Storr AH, Ansorge O, et al: Dopamine transporter imaging for the diagnosis of dementia with Lewy bodies. *Cochrane Database Syst Rev* 1: CD010633, 2015.
11) Oinas M, Polvikoski T, Sulkava R, Myllykangas L, Juva K, et al: Neuropathologic findings of dementia with lewy bodies (DLB) in a population-based Vantaa 85+study. *J Alzheimers Dis* 18: 677−689, 2009.
12) Jellinger KA, Attems J: Prevalence and pathology of dementia with Lewy bodies in the oldest old: A comparison with other dementing disorders. *Dement Geriatr Cogn Disord* 31: 309−316, 2011.
13) Bousiges O, Blanc F: Diagnostic value of cerebro-spinal fluid biomarkers in dementia with lewy bodies. *Clin Chim Acta* 490: 222−228, 2019.
14) Vermeiren Y, Van Dam D, Aerts T, Engelborghs S, Martin JJ: The monoaminergic footprint of depression and psychosis in dementia with Lewy bodies compared to Alzheimer's disease. *Alzheimers Res Ther* 7: 7, 2015.
15) Janssens J, Vermeiren Y, Fransen E, Aerts T, Van Dam D, et al: Cerebrospinal fluid and serum MHPG improve Alzheimer's disease versus dementia with Lewy bodies differential diagnosis. *Alzheimers Dement* 10: 172−181, 2018.
16) Tsutsui H, Muguruma Y, Noda T, Akatsu H, Matsukawa N, et al: Development of targeted metabolomics for the determination of ornithine cycle compounds as possible biomarkers in cerebrospinal fluid regarding to Alzheimer's disease pathology using UHPLC-ESI-MS/MS. *Med Mass Spectrometry* 2: 11−20, 2018.
17) Nagatomo R, Okada Y, Ichimura M, Tsuneyama K, Inoue K: Application of 2-picolylamine derivatized ultra-high performance liquid chromatography tandem mass spectrometry for the determination of short-chain fatty acids in feces samples. *Anal Sci* 34: 1031−1036, 2018.
18) Chen Z, Gao Z, Wu Y, Shrestha R, Imai H, et al: Development of a simultaneous quantitation for short-, medium-, long-, and very long-chain fatty acids in human plasma by 2-nitrophenylhydrazine-derivatization and liquid chromatography-tandem mass spectrometry. *J Chromatogr: B* 1126−1127: 121771, 2019.
19) Xiao HM, Wang X, Liao QL, Zhao S, Huang WH, et al:

Sensitive analysis of multiple low-molecular-weight thiols in a single human cervical cancer cell by chemical derivatization-liquid chromatography-mass spectrometry. *Analyst* 144: 6578−6585, 2019.

20) Sánchez-López E, Crego AL, Marina ML: Design of strategies to study the metabolic profile of highly polar compounds in plasma by reversed-phase liquid chromatography-high resolution mass spectrometry. *J. Chromatogr. A* 1490: 156−165, 2017.
21) Muguruma Y, Tsutsui H, Noda T, Akatsu H, Inoue K: Widely targeted metabolomics of Alzheimer's disease postmortem cerebrospinal fluid based on 9-fluorenylmethyl chloroformate derivatized ultra-high performance liquid chromatography tandem mass spectrometry. *J Chromatogr B* 1091: 53−66, 2018.
22) Shen L, Thompson PM, Potkin SG, Bertram L, Farrer LA, et al: Genetic analysis of quantitative phenotypes in AD and MCI: Imaging, cognition and biomarkers. *Brain Imaging Behav* 8: 183−207, 2014.
23) Huynh RA, Mohan C: Alzheimer's disease: Biomarkers in the genome, blood, and cerebrospinal fluid. *Front Neurol* 8: 102, 2017.
24) Wishart DS, Feunang YD, Marcu A, Guo AC, Liang K, et al: HMDB 4.0: The human metabolome database for 2018. *Nucleic Acids Res* 46: D608-D617, 2018.
25) Kanehisa M, Furumichi M, Tanabe M, Sato Y, Morishima K: KEGG: New perspectives on genomes, pathways, diseases and drugs. *Nucleic Acids Res* 45: D353-D361, 2017.
26) Tsuruoka M, Hara J, Hirayama A, Sugimoto M, Soga T, et al: Capillary electrophoresis-mass spectrometry-based metabolome analysis of serum and saliva from neurodegenerative dementia patients. *Electrophoresis* 34: 2865−72, 2013.
27) Hata J, Ohara T, Katakura Y, Shimizu K, Yamashita S, et al: Association between serum β-alanine and risk of dementia. *Am J Epidemiol* 188: 1637−1645, 2019.
28) Saransaari P, Oja SS: Beta-alanine release from the adult and developing hippocampus is enhanced by ionotropic glutamate receptor agonists and cell-damaging conditions. *Neurochem Res* 24: 407−414, 1999.
29) Hipkiss AR, Brownson C: A possible new role for the anti-ageing peptide carnosine. *Cell Mol Life Sci* 57: 747−753, 2000.
30) Milioni F, de Poli RAB, Saunders B, Gualano B, da Rocha AL, et al: Effect of β-alanine supplementation during high-intensity interval training on repeated sprint ability performance and neuromuscular fatigue. *J Appl Physiol* 127: 1599−1610, 2019.
31) Saunders B, Elliott-Sale K, Artioli GG, Swinton PA, Dolan E, et al: β-Alanine supplementation to improve exercise capacity and performance: A systematic review and meta-analysis. *Br J Sports Med* 51: 658−669, 2017.
32) Madine J, Wang X, Brown DR, Middleton DA: Evaluation of beta-alanine- and GABA-substituted peptides as inhibitors of disease-linked protein aggregation. *Chembiochem* 10: 1982−1987, 2009.